

LAND-USE FILTERING FOR NONSTATIONARY SPATIAL PREDICTION OF COLLECTIVE EFFICACY IN AN URBAN ENVIRONMENT

BY J. BRANDON CARTER^{1,a} , CHRISTOPHER R. BROWNING^{2,c} , BETHANY BOETTNER^{3,e} , NICOLO PINCHAK^{2,d} , AND CATHERINE A. CALDER^{1,b} 

¹Department of Statistics and Data Sciences, University of Texas at Austin, ^acarterjb@utexas.edu; ^bcalder@austin.utexas.edu

²Department of Sociology, The Ohio State University, ^cbrowning.90@osu.edu; ^dpinchak.5@osu.edu

³Population Research Institute, The Ohio State University, ^eboettner.6@osu.edu

Collective efficacy – the capacity of communities to exert social control toward the realization of their shared goals – is a foundational concept in the urban sociology and neighborhood effects literature. Traditionally, empirical studies of collective efficacy use large sample surveys to estimate collective efficacy of different neighborhoods within an urban setting. Such studies have demonstrated an association between collective efficacy and local variation in community violence, educational achievement, and health. Unlike traditional collective efficacy measurement strategies, the Adolescent Health and Development in Context (AHDC) Study implemented a new approach, obtaining spatially-referenced, place-based ratings of collective efficacy from a representative sample of individuals residing in Columbus, OH. In this paper, we introduce a novel nonstationary spatial model for interpolation of the AHDC collective efficacy ratings across the study area which leverages administrative data on land use. Our constructive model specification strategy involves dimension expansion of a latent spatial process and the use of a filter defined by the land-use partition of the study region to connect the latent multivariate spatial process to the observed ordinal ratings of collective efficacy. Careful consideration is given to the issues of parameter identifiability, computational efficiency of an MCMC algorithm for model fitting, and fine-scale spatial prediction of collective efficacy.

1. Introduction. For decades, social science research has investigated how neighborhood residents can mobilize to address local problems (Shaw and McKay, 1942; Jacobs, 1961). The theory of neighborhood collective efficacy has been highly influential in this respect (Sampson, Raudenbush and Earls, 1997). Uniting Coleman’s (1988) concept of social capital and Bandura’s (1982; 1986) research on personal and group-level self-efficacy, neighborhood collective efficacy is a construct capturing the collective capacity of community members to exert social control toward the realization of their shared goals (e.g., low levels of crime).

Empirical tests of the neighborhood collective efficacy theory often rely on data collected through sample surveys administered to residents of different neighborhoods within an urban center. Collective efficacy survey instruments vary, but typically ask urban residents to report perceptions of local trust, monitoring, and intervention norms in their neighborhood. We refer to these three categories of questions – “trust,” “observation,” and “defense,” respectively – as the *components* of collective efficacy. Reports on these components are then aggregated within geographic units consistent with the notion of neighborhoods (e.g., census tracts). For example, the Project on Human Development in Chicago Neighborhoods (PHDCN), conducted in the mid 1990s, used neighborhood ratings from nearly 8,000 Chicago residents

Keywords and phrases: Bayesian statistics, Data augmentation, Dimension expansion, Nonstationarity, Sociology, Spatial statistics.

clustered within 343 census-based neighborhoods to capture collective efficacy (Raudenbush and Sampson, 1999; see also Matsueda and Drakulich, 2016; Wickes et al., 2019). In the PHDCN and other studies, multilevel/hierarchical regression models were used to capture between-neighborhood variation in collective efficacy through random effects, which are assumed to be spatially independent or dependent over the study region depending on the study design. control (i.e., the presence of “eyes on the street” (Jacobs, 1961)). Studies of neighborhood-level collective efficacy have found inverse associations with a host of neighborhood problems such as rates of homicide (Sampson, Raudenbush and Earls, 1997), intimate partner violence (Browning, 2002), child maltreatment (Molnar et al., 2015), and chronic disease (Cohen et al., 2006), even after adjusting for neighborhood sociodemographic factors.

In this paper, we extend the notion of collective efficacy as a continuously-indexed spatial feature of an urban area, which is defined by the collective impressions of places individuals visit as part of their normal, everyday routine. Using point-referenced collective efficacy data collected as part of the Adolescent Health and Development in Context (AHDC) Study, described in detail in Section 2, we estimate the components of collective efficacy across the city of Columbus, OH. Our approach also uses taxation-based records on the land use of parcels – small geographic units often used as a proxy for a “place.” Consistent with recent work suggesting that land-use compositions affect the levels of collective efficacy within neighborhoods (Corcoran et al., 2018), we use the category of land use to model spatial variation in the mean of the collective efficacy component processes. Our novel contribution from a statistical perspective is that we capture land-use driven (i.e. driven by spatially-referenced covariate information), second-order nonstationarity through a dimension-expansion strategy, building upon existing approaches for covariate-driven nonstationary spatial modeling (Calder, 2008; Schmidt, Guttorp and O’Hagan, 2011; Reich et al., 2011; Neto, Schmidt and Guttorp, 2014; Ingebrigtsen, Lindgren and Steinsland, 2014; Risser and Calder, 2015; Risser et al., 2019). In a similar spirit to the dimension expansion approach to nonstationary spatial modeling of Bornn, Shaddick and Zidek (2012), we augment the dimension of the latent collective efficacy component processes to the number of land-use categories and model a multivariate, stationary spatial process as if spatially-referenced data on land-use specific collective efficacy components were observable everywhere. We then relate the observations to the higher dimensional random process using a filter defined by the land-use partitioned study area. We show that our land-use filtering model provides a better fit to the AHDC collective efficacy data than a traditional spatial generalized linear mixed model with a single latent second-order stationary Gaussian process (Banerjee, Carlin and Gelfand, 2014).

Our proposed methodology advances the measurement of collective efficacy in two ways. First, it is compatible with the more cost effective data collection strategy employed in the AHDC Study, where study participants report on collective efficacy levels at their routine activity locations, of which most have between five and eight. In addition, our model readily allows point-level prediction of the components of collective efficacy across the entire study area to better understand within neighborhood variation in collective efficacy. Point-level variability in collective efficacy may help explain phenomena such as crime which has been shown to concentrate at particular locations within neighborhoods (Weisburd et al., 2016). Finally, we note that while developed for the study of collective efficacy, our methodology can be readily applied in other spatial prediction settings where the study area can be partitioned into an arbitrary number of land-use categories.

The outline of the paper is as follows. In Section 2, we introduce the AHDC Study and the collective efficacy data. In addition, we describe exploratory analyses of the data that motivate our novel land-use filtering methodology. Section 3 introduces our land-use filtering

model and details land-use filtering as applied to our ordinal response variable. We provide a summary of inferences and predictions from our fitted model to the AHDC data in Section 4 and discuss implications of our modeling and data collection choices in Section 5.

2. Data and exploratory analyses. In this section, we describe the AHDC data in more detail and visually summarize the spatial patterning of the ratings of the components of collective efficacy. We also introduce the land-use data, which drives our proposed spatial filtering strategy for smoothing the ratings across the study area. This section concludes with summaries of preliminary models that motivate the more complex modeling strategy introduced in Section 3.

2.1. AHDC data. The AHDC Study is a longitudinal data collection project designed to improve understanding of how social, psychological, and biological processes shape youth developmental outcomes. Participants in the study are members of a representative sample of households with youth aged 11 to 17 residing within the I-270 belt loop in Franklin County, OH, which contains the city of Columbus and some of its interior suburbs. In this paper, we use data from AHDC Wave 1, which was collected between 2014-2016. For each sampled household, one randomly-sampled youth aged 11-17 was selected for participation in the study. Upon enrollment, the primary caregiver, typically, but not always, the mother of the enrolled youth, filled out an entrance questionnaire which included questions on family and household composition, alcohol and substance use, employment and income, health, and social support. In addition to answering these demographic and socioeconomic background questions, caregivers also listed locations they frequent as part of their everyday routine. Caregivers indicated the location type (e.g. home, kid's school, friends' and relatives' houses, work, grocery stores, etc.) and when they typically spend time at the location (e.g. daytime, nighttime, weekdays, weekends). They also answered multiple questions on each reported location to assess the social climate. These location ratings are the key data used in this current analysis to understand spatial variation in collective efficacy. From the location assessments, we focus on three collective efficacy questions posed as statements to which the caregiver rated agreement on a five-point Likert scale: *If someone was being threatened near [location], other people around would come to their defense.* *You can trust people on the streets in the area near [location].* *There are usually people watching what's happening in the area near [location].*¹ We refer to the responses to these questions and their corresponding latent spatial processes, respectively, as "defense," "trust," and "observation". While location ratings outside of the study area were provided, we restrict our analysis to the 4526 locations within the I-270 belt loop. Out of the 1369 caregivers in the data set, the number of reports by a single caregiver ranged from 1 to 27, with an average of 6.8 reports. With a few exceptions², all reports included ratings on all three components of collective efficacy along with time of day the location is visited (daytime, nighttime, or both) and day of week (weekday, weekend, or both). Caregivers were asked to rate their home location for both daytime and nighttime separately.

¹The first two statement had response options "strongly agree," "agree," "neither agree nor disagree," "disagree," and "strongly disagree," while the last statement had responses "never," "almost never," "sometimes," "fairly often" and "very often." Each response was displayed in the order listed above next to the corresponding numeric value 1-5. In fitting the model we recoded the responses so that 1 corresponded to the least affirmative value (never or strongly disagree) and 5 the most affirmative value (very often and strongly agree) for all three components.

²Due to a technical error in the administration of the survey, the question about trust was omitted from the initial surveys resulting in fewer ratings for the trust component as compared to defense and observation.

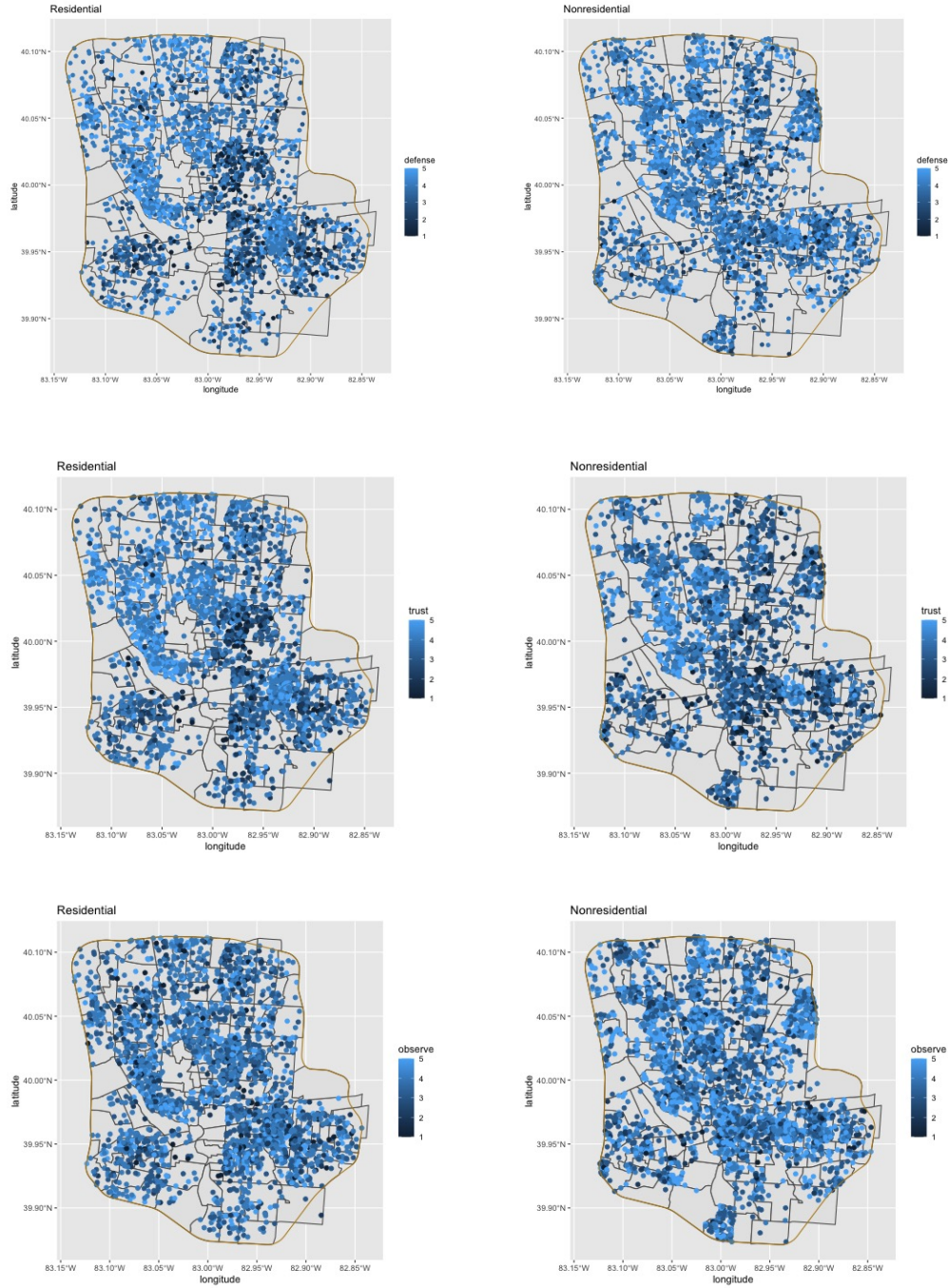


FIG 1. Survey responses for the defense (top row), trust (middle row), and observation (bottom row) components plotted for residential locations (left column) and nonresidential locations (right column). The gray lines show census tract boundaries and the orange line is the 270 belt loop. Rated locations have been jittered within Census block group to preserve the anonymity of study participants. Due to the jittering, some locations are plotted outside the I-270 belt loop. The plots were created in R ([R Core Team, 2022](#); [Pebesma, 2018](#); [Wickham et al., 2019](#)).

Figure 1 shows the locations to which the ratings of defense, trust, and observation correspond, plotted separately for residential and nonresidential locations (as derived from the caregiver’s report on the location type). For the defense responses, the residential ratings appear to show strong spatial dependence. The northwest quadrant and a pocket of residences in the central east exhibit clusters of higher ratings for defense, with lower ratings of defense elsewhere. Nonresidential locations also appear to exhibit the same general spatial patterning, yet this pattern is much less visually pronounced than it is for residential locations. The difference in the spatial patterns for defense ratings between residential and nonresidential locations seems to indicate that the ratings arise from two different, yet correlated, spatial processes. Thus, we cannot entirely account for the difference between ratings in residential and nonresidential locations by assuming a stationary univariate spatial process for defense ratings while controlling for location type in the mean function.

A similar pattern is evident in Figure 1 for the trust and observation components in that the spatial patterns of ratings for residential and nonresidential locations are distinct. For the trust component (middle row), higher ratings in the upper right quadrant extend over a larger area for residential locations as compared to nonresidential locations where the high ratings are more localized. For trust, both residential and nonresidential ratings appear to show strong spatial dependence, but the strength of spatial dependence is not the same across location types. The observation ratings (bottom row) visually show less of a distinctive spatial pattern. It is difficult from visual inspection of these maps alone to draw conclusions about the underlying spatial process that gives rise to the observation ratings across residential and nonresidential locations. Yet, for all three components, it appears that allowing only the mean to vary spatially cannot fully account for the differences in the spatial patterning of observed ratings in residential and nonresidential locations.

2.2. Land-use data. In order to account for the effects of land use on differences in the spatial dependence structure of the components of collective efficacy across the study region when predicting collective efficacy components at unrated location, we require the land-use designation of all prediction locations, which is not available in the AHDC data. In particular, caregivers’ reported location types are straightforward to classify as residential and nonresidential, however, we need an objective and systematic method to categorize all other locations in the study area not reported on. To this end, we utilized the May 2014 parcel data for the study area, downloaded from the Franklin County Auditor’s publicly accessible FTP site ([Franklin County Auditor, 2021](#)). Each parcel has a designated tax code which we classified into one of three categories: residential, nonresidential, and other. We introduce the “other” category to distinguish nonresidential locations with minimal social presence, such as warehouses, quarries, parking lots and industrial centers, from locations where a social presence is expected. Figure 2 shows the partition of the study area into residential, nonresidential, and other categories as informed by the taxcodes of the parcel data. Most locations in the AHDC data lie within the boundaries of a parcel and received the same classification as the parcel within which they lie. The coordinates of other AHDC-reported locations fall on the road network and do not lie within the boundaries of a parcel. For these locations we assigned the land-use category of the nearest parcel. After initial assignments were made, we performed a second sweep of the data to verify that the reported caregiver location type matched the assigned parcel land-use type. Incongruencies existed between reported location types and assigned land-use types (e.g. location reported by caregiver as “neighborhood,” but assigned to parcel with tax designation “warehouse” and land-use category “other”). For such locations we reassigned the land-use category if any of the next 5 nearest parcels had a tax code and land-use assignment that was coherent with the reported location type. We deemed locations without a nearby congruent parcel as a reporting error and did not include them in the analysis. Table 1 gives the total number of ratings and locations used in our analysis broken down by collective efficacy component and land-use category.

TABLE 1

Breakdown of the number of locations, m , and ratings, n , by collective efficacy component. The subscripts on m and n further breakdown location and ratings counts by land-use type, with 1 for residential, 2 for nonresidential and 3 for “other”.

	Defense	Trust	Observation
m	3867	3040	3826
m_1	1770	1555	1777
m_2	2045	1447	1997
m_3	52	38	52
n	7580	5865	7548
n_1	2906	2653	2917
n_2	4616	3170	4573
n_3	58	42	58

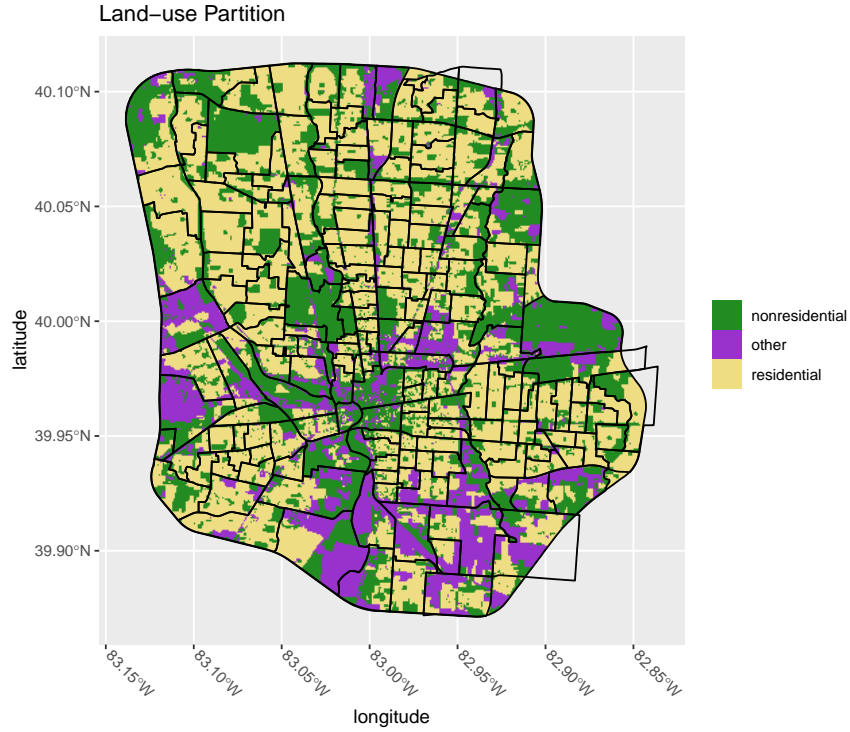


FIG 2. Partition of the study region into land-use categories. Each cell color is determined by the tax code of the nearest parcel

2.3. Preliminary exploratory modeling. To better understand the difference in spatial variation in collective efficacy components by land-use categories, we fit separate univariate Bayesian spatial ordinal regression models to each component of collective efficacy by land-use category (excluding the “other” category which has only approximately 50 ratings for each component). That is, we fit six models corresponding to the three components of collective efficacy (defense, trust, and observation) by the two land-use categories (residential and

nonresidential, as determined by the parcel data). Section 3 provides details on the specification of spatial ordinal regression models, but here we focus on inferences of key parameters describing the nature of the spatial dependence as a justification for our proposed model. Let $\theta = (\phi, \tau^2)$ be the vector of spatial dependence parameters characterizing the exponential covariance function of the latent spatial process, where ϕ represents the spatial range and τ^2 is the parameter that governs the proportion of variance due to spatial variation, as opposed to independent error (in the Bayesian ordinal regression model the variance of the independent error is fixed at one). For all models, we adjust for the time-of-day (daytime, nighttime, or both) and the day-of-week (weekday only, weekend only, or mixed) variables in the mean function as indicated by the caregiver in the survey response. We obtained draws from the posterior distribution using the MCMC scheme described in Section 3.5.1.

TABLE 2

Estimates of the marginal posterior mean of the covariance parameters from Bayesian spatial ordinal models for the defense, trust, and observation components fitted separately to the residential and nonresidential ratings.

	Defense		Trust		Observation	
	ϕ	τ^2	ϕ	τ^2	ϕ	τ^2
Residential	334.29	2.08	443.68	3.03	2156.17	2.06
Nonresidential	53.28	0.15	42.63	0.48	77.02	0.16

Table 2 shows the estimated mean of the marginal posterior distribution of the spatial range parameter, ϕ , and spatial proportion-of-variance parameter, τ^2 , for all six fitted preliminary models. The parameter estimates for the models fitted to the residential data differ from the estimates from the nonresidential data across all three collective efficacy components. A higher value of ϕ indicates a shorter range of spatial dependence and a high value of τ^2 indicates a larger proportion of the variance is attributed to the spatial dependence rather than independent random error. Across all three components, nonresidential locations have longer range spatial dependence, but show greater variation within location. We plot the estimated posterior mean correlation function with 95% pointwise credible intervals in Figure 3. For each pair of posterior samples of ϕ and τ^2 , we calculated the correlation function for a grid of distances from 0 to 5 miles and plot the pointwise mean and lower/upper bounds of a 95% credible interval. For the defense component, the correlation function for the residential data is characterized by shorter term spatial dependence with an effective range of a little less than a mile and roughly .6 of the variation attributable to spatial dependence. In contrast, the correlation function for the nonresidential data of the defense component has an effective range of roughly 3 miles and a much larger proportion of independent error. A similar pattern characterizes the difference between the correlation functions for the trust and observation components. The difference in the estimated correlation functions between the two types of locations suggests that a model which accounts for the difference in spatial dependence between locations of different land-use types will better capture the overall spatial dependence structure of the data.

The spatial dependence structure of the model has implications for the main goal of our analysis: to predict levels of each component of collective efficacy at unobserved locations. A spatial generalized linear mixed model with a single latent stationary spatial process would most likely lead to an estimated correlation function somewhere between the two distinct correlation functions shown in Figure 3. We show this is indeed the case in Section 4 for all three components of collective efficacy. By expanding the dimension of the response to include a latent spatial process for each land-use type, we can estimate the spatial range of each land-use process. This will allow us to have a better understanding of the spatial process

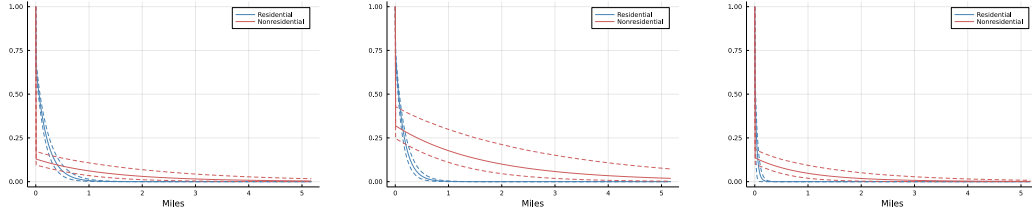


FIG 3. *Estimated posterior mean correlation functions from Bayesian spatial ordinal models for residential and nonresidential locations of the defense, trust, and observation component, plotted respectively from left to right. Dashed lines indicate lowers and upper bounds of 95% posterior point-wise credible intervals.*

of each component of collective efficacy at a finer resolution within census tract or block group. Furthermore, we can smooth over land-use boundaries through the cross correlations between the latent processes corresponding to land-use types.

3. Land-use filtering model. In this section, we introduce a novel land-use filtering model, a Bayesian spatial generalized linear model that incorporates a dimension expansion and multivariate spatial modeling strategies. We begin with a motivating schematic to demonstrate how land-use filtering captures nonstationarity behavior in a latent univariate spatial process. Throughout this section we omit notation references the three different components of collective efficacy since we will fit the same model to each component separately.

3.1. Motivation. When the study area can be partitioned into different land-use categories (or some other spatial partition), we can expand the dimension of the latent spatial process in a spatial generalized linear mixed model to allow distinct spatial dependence structures for each land-use category. To motivate the land-use filtering model developed formally in the next section, consider the following generative model illustrated in Figure 4. We generate from a mean-zero latent multivariate spatial process with a known cross-covariance function on a fine grid of locations distributed across a two-dimensional region (a unit square in Figure 4). The assumed marginal spatial correlation functions for this illustrative example are shown on the left panel. We then discard the components of each sample that do not correspond to the land-use category of a particular location, producing the top three plots in the center column of Figure 4. The bottom plot shows the filtered process created by combining the land-use specific component processes at each location. The resulting image is fairly locally smooth across land-use boundaries due to the cross-component dependence of the latent process, but the spatial dependence structure is not uniform across space. Lastly, we assign an ordinal rating to a set of random locations within the study area based on the value of the latent process at the locations. That is, these ratings are based on the non-discarded component of the simulated random vector associated with that location (top three plots on the right column). The simulated ratings (bottom right) arising from the filtered latent process (bottom center) are analogous to the AHDC collective efficacy ratings.

Note that in Figure 4 when the ratings across all three land-use categories are plotted together (bottom right column), it is difficult to visualize different covariance structures which are (more) distinguishable when the latent processes are plotted together. By expanding the univariate response to allow for distinct spatial correlation functions for each land-use category and dependence across land-use categories, we can improve model fit for the AHDC collective efficacy ratings.

3.2. Land-use filtering ordinal regression. In specifying our land-use filtering model, we consider only a single component of collective efficacy. Each of the AHDC caregivers

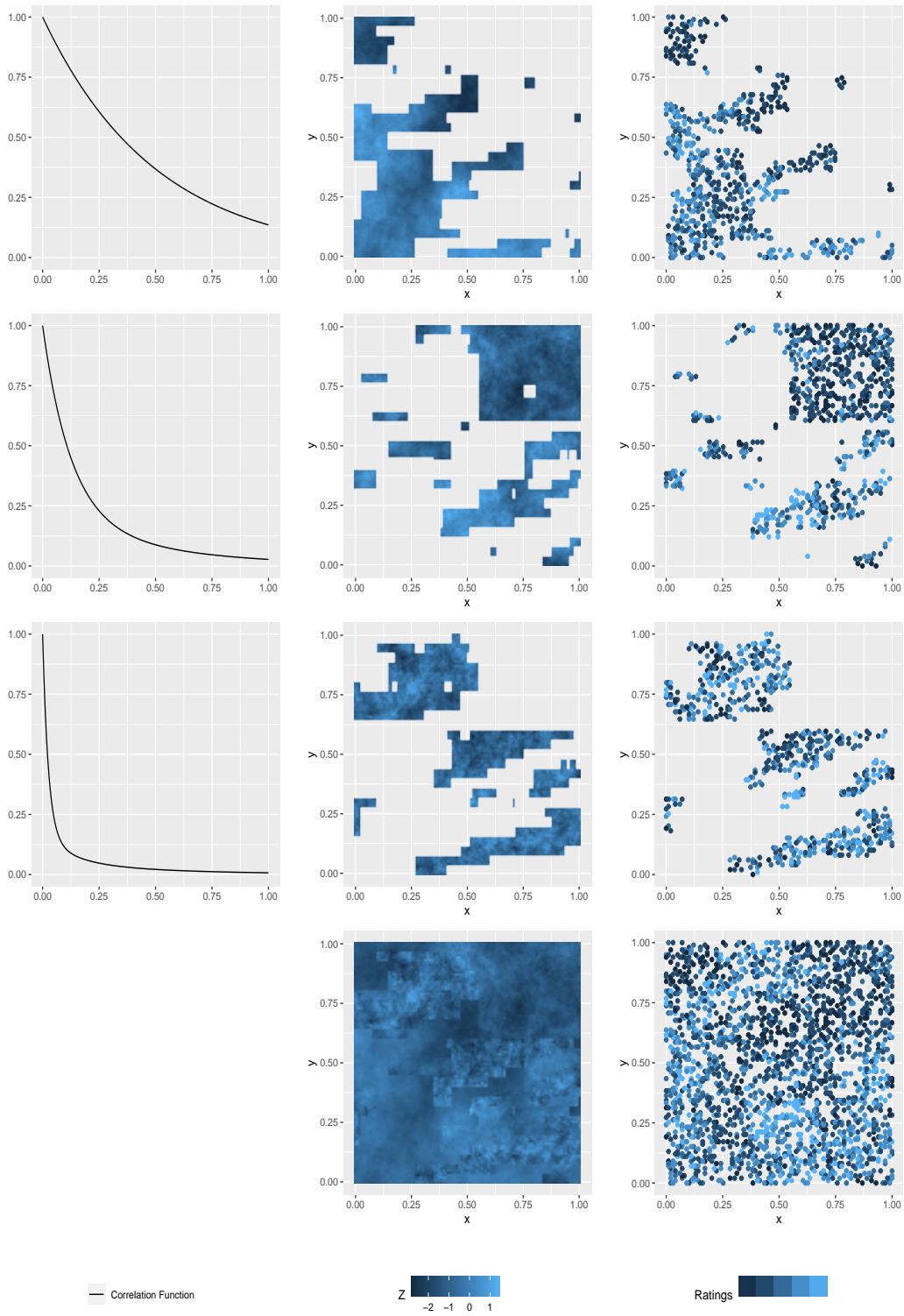


FIG 4. A demonstration of a generative model for ordinal data under land-use filtering. See Section 3.1 for a discussion.

provides their rating on a five-point ordinal scale, where a rating of $K \equiv 5$ is the “best” and 1 is the “worst.” To facilitate specification of our model, we introduce notation for the ratings, with the primary index indicating the location of the rating. We let Y_{ij} denote the j th rating of the i th location, where s_i is a unique location in the study area, \mathcal{S} , for $i = 1, \dots, m$ and $j = 1, \dots, n_i$. The constant m is the number of unique locations, and n_i is the total number of caregivers who rated on i th location. We denote the total number of ratings as $n = \sum_{i=1}^m n_i$, and the collection of all ratings as $\mathcal{Y} = \{Y_{ij} : i = 1, \dots, m; j = 1, \dots, n_i\}$.

We model the elements of \mathcal{Y} using a Bayesian ordinal probit regression model, specified using the well known data augmentation scheme of [Albert and Chib \(1993, 1997\)](#), which has been extended to the spatial setting by [De Oliveira \(1997, 2000\)](#); [Higgs and Hoeting \(2010\)](#); [Schliep and Hoeting \(2015\)](#); [Berrett and Calder \(2012, 2016\)](#). Under this scheme, we introduce continuous latent variables Z_{ij}^* defined at each of the m locations and for each n_i ratings and unknown cut points, $\gamma_1, \dots, \gamma_{K-1}$ such that

$$Y_{ij} = \begin{cases} K & \text{if } \gamma_{K-1} < Z_{ij}^* \\ k & \text{if } \gamma_{k-1} < Z_{ij}^* < \gamma_k, \text{ for } k = 2, \dots, K-1. \\ 1 & \text{if } Z_{ij}^* < \gamma_1 \end{cases}$$

Unlike the setting discussed in [Higgs and Hoeting \(2010\)](#), we have multiple latent random variables defined at each location due to the fact that some locations are rated by multiple individuals. Each of these random variables is related to a single latent spatial process $\tilde{Z}(\mathbf{s})$ defined for all $\mathbf{s} \in \mathcal{S}$. We assume that the Z_{ij}^* s are conditionally independent given the latent spatial process $\tilde{Z}(\mathbf{s}_i)$, and parameters β , θ , and σ^2 :

$$Z_{ij}^* | \tilde{Z}(\mathbf{s}_i), \beta, \theta, \sigma^2 \sim N(\mathbf{x}_{ij}'\beta + \tilde{Z}(\mathbf{s}_i), \tilde{\sigma}_{g(\mathbf{s}_i)}^2).$$

Here, \mathbf{x}_{ij} is a $p \times 1$ vector of covariates associated with the j th rating of location i and β is the corresponding $p \times 1$ vector of regression coefficients. The vector $\tilde{\sigma}^2$ contains the variance parameters for the independent error of each land-use process and $g(\mathbf{s}) : \mathcal{S} \rightarrow \{1, \dots, Q\}$ is a function that returns the index of the land-use category of location \mathbf{s} . We use the tilde notation to highlight the fact that this latent process is constrained so that the total error variance of the Z_{ij}^* s is equal to one. Constraining the latent spatial process in ordinal regression model aids in the identifiability of the covariance parameters θ ([Yan et al., 2007](#)). We discuss additional identifiability considerations for spatial ordinal regression models Section 3.3. The vector θ denotes the covariance parameters associated with the spatial process $\tilde{Z}(\mathbf{s})$, on which $\tilde{\sigma}^2$ also depends, due to the constraint on the total error variance of Z_{ij}^* .

Before defining the constrained $\tilde{Z}(\mathbf{s})$ and a model for its unconstrained analogue $Z(\mathbf{s})$, we introduce a Q -dimensional spatial process $\eta(\mathbf{s})$, where Q is the number of land-use categories in the spatial partition. We define $\eta(\mathbf{s})$ to be a multivariate Gaussian process with mean zero and parametric covariance function $\Sigma_{\mathbf{s}, \mathbf{s}'}^{(\eta)}(\theta)$ defined by the linear model of coregonalization (LMC). The LMC remains the standard approach to create covariance functions in multivariate spatial modeling ([Goulard and Voltz, 1992](#); [Grzebyk and Wackernagel, 1994](#); [Wackernagel, 2003](#); [Gelfand et al., 2004](#)). While alternatives to the LMC exist (e.g., [Gneiting, Kleiber and Schlather \(2010\)](#) and [Apanasovich, Genton and Sun \(2012\)](#) propose Matérn cross-covariance functions for multivariate random fields), [De Oliveira \(1997, 2000\)](#) have shown that smoothness parameters (such as the smoothness parameter in the Matérn covariance function) are near nonidentifiable in spatial ordinal regression models. Since our η will be a component of a spatial ordinal regression model, we prefer the LMC specification.

The LMC is a constructive approach for modeling a multivariate spatial process as a linear combination of independent spatial processes. Let $\mathbf{w}(\mathbf{s})$ be a Q -dimensional spatial process comprised of independent component processes $\mathbf{w}_1, \dots, \mathbf{w}_Q(\mathbf{s})$. Each $\mathbf{w}_q(\mathbf{s})$ is a Gaussian

process with mean 0, variance 1, and correlation function $\rho_q(\mathbf{s}, \mathbf{s}'; \phi_q)$, where ϕ_q are unknown parameters. Again, since smoothness parameters are near nonidentifiable, we specify $\rho_q(\mathbf{s}, \mathbf{s}'; \phi_q)$ as an exponential correlation function,

$$\rho_q(\mathbf{s}, \mathbf{s}', \phi_q) = \exp(-\phi_q \|\mathbf{s} - \mathbf{s}'\|),$$

but note that alternate correlation functions could be used instead. In the LMC specification, we assume that $\boldsymbol{\eta}(\mathbf{s}) = \mathbf{A}\mathbf{w}(\mathbf{s})$, where \mathbf{A} is a $Q \times Q$ lower triangular matrix with $Q \times (Q - 1)/2$ unknown parameters. It follows directly that the cross covariance for $\boldsymbol{\eta}(\mathbf{s})$ and $\boldsymbol{\eta}(\mathbf{s}')$ is

$$\boldsymbol{\Sigma}_{\mathbf{s}, \mathbf{s}'}^{(\boldsymbol{\eta})}(\boldsymbol{\theta}) = \mathbf{A}\boldsymbol{\Gamma}(\mathbf{s}, \mathbf{s}')\mathbf{A}',$$

where $\boldsymbol{\theta}$ consists of the elements of $\boldsymbol{\phi}$ and unknown elements of \mathbf{A} and $\boldsymbol{\Gamma}(\mathbf{s}, \mathbf{s}')$ is a matrix valued function with $\rho_q(\mathbf{s}, \mathbf{s}', \phi_q)$ on the q th diagonal.

We now relate the Q -dimensional process $\boldsymbol{\eta}(\mathbf{s})$ to the univariate process $Z(\mathbf{s})$ using land-use filtering (i.e., extracting the component of $\boldsymbol{\eta}(\mathbf{s})$ corresponding to the land-use category of \mathbf{s}). Formally, we define

$$Z(\mathbf{s}) = f(\boldsymbol{\eta}(\mathbf{s}), g(\mathbf{s})) = \eta_{g(\mathbf{s})}(\mathbf{s}) + \delta_{g(\mathbf{s})},$$

where $\boldsymbol{\delta} = (\delta_1, \dots, \delta_Q)$ is a vector of unknown mean shift parameters defining the mean of the $Z(\mathbf{s})$ process. Writing $Z(\mathbf{s}) = \mathbf{a}'_q \mathbf{w}(\mathbf{s}) + \delta_q$, it is clear that $Z(\mathbf{s})$ is a Gaussian process with mean function $\delta(\mathbf{s})$, where

$$\delta(\mathbf{s}) = \delta_{g(\mathbf{s})},$$

and cross-covariance function

$$\boldsymbol{\Sigma}_{\mathbf{s}, \mathbf{s}'}^{(Z)}(\boldsymbol{\theta}) = \mathbf{a}'_{g(\mathbf{s})} \boldsymbol{\Gamma}(\mathbf{s}, \mathbf{s}') \mathbf{a}_{g(\mathbf{s}')}.$$

between any two locations \mathbf{s} and \mathbf{s}' with land-use types $g(\mathbf{s})$ and $g(\mathbf{s}')$. Note that $Z(\mathbf{s})$ is nonstationary with both a mean function $\delta(\mathbf{s})$ and covariance function $\boldsymbol{\Sigma}_{\mathbf{s}, \mathbf{s}'}^{(Z)}(\boldsymbol{\theta})$ that vary across land-use categories.

To complete the specification of the model, we need to define the covariance function for the constrained $\tilde{Z}(\mathbf{s})$, which allow the Z_{ij}^* s to have total variance of one. First we note that the variance of the unconstrained, land-use-category-specific process $\eta_q(\mathbf{s}) + \delta_q$ is $\|\mathbf{a}_q\|^2$, where \mathbf{a}_q is the q th row of \mathbf{A} . It follows then that the constrained covariance is

$$(1) \quad \tilde{\boldsymbol{\Sigma}}_{\mathbf{s}, \mathbf{s}'}^{(\tilde{Z})}(\boldsymbol{\theta}^*) = \frac{\mathbf{a}'_{g(\mathbf{s})} \boldsymbol{\Gamma}(\mathbf{s}, \mathbf{s}') \mathbf{a}_{g(\mathbf{s}')}}{\sqrt{\|\mathbf{a}_{g(\mathbf{s})}\|^2 + \sigma_{g(\mathbf{s})}^2} \sqrt{\|\mathbf{a}_{g(\mathbf{s}')} \|^2 + \sigma_{g(\mathbf{s}')}^2}},$$

where $\boldsymbol{\theta}^* = \{\text{vec}(\mathbf{A}), \boldsymbol{\phi}, \boldsymbol{\sigma}^2\}$. Additionally, the independent errors are also constrained so that

$$\tilde{\sigma}_{g(\mathbf{s})}^2 = \frac{\sigma_{g(\mathbf{s})}^2}{\|\mathbf{a}_{g(\mathbf{s})}\|^2 + \sigma_{g(\mathbf{s})}^2}.$$

The resulting constrained process, $\tilde{Z}(\mathbf{s})$, is a nonstationary Gaussian process

$$\tilde{Z}(\mathbf{s}) | \delta(\mathbf{s}), \boldsymbol{\theta}^* \sim \text{GP}(\delta(\mathbf{s}), \tilde{\boldsymbol{\Sigma}}_{\mathbf{s}, \mathbf{s}'}^{(\tilde{Z})}(\boldsymbol{\theta}^*)),$$

with mean function $\delta(\mathbf{s})$ and covariance function $\tilde{\boldsymbol{\Sigma}}_{\mathbf{s}, \mathbf{s}'}^{(\tilde{Z})}(\boldsymbol{\theta}^*)$.

3.3. Identifiability of model parameters. By augmenting our data with the latent variables Z^* s, we are able to estimate the latent spatial process $\tilde{Z}(s)$; however, as the observed data is discrete, there is not enough information in the data to identify all parameters that define the latent spatial process in the augmented space, which is continuous.

First, a global intercept (or cell means intercepts) is confounded with the cut points γ . To address this confounding we fix $\delta_1 = 0$, the mean of the first land-use process and estimate the remaining δ_q for $q > 1$. Additionally, we exclude a global intercept from β , the vector of regression coefficients. Alternatively, one could fix one of the cut points, for example $\gamma_1 = 0$, which would allow the estimation of a global intercept in β or the estimation of δ_1 , but not both. As a last consideration on the cut points, in a standard multivariate probit model, one could use a different set of cut points for each multivariate process. We opt for the same set of cut points across the land-use processes so that interpretation of the latent variable $\tilde{Z}(s)$ is consistent across land-use categories.

In the model specified above, the constrained covariance $\tilde{\Sigma}_{s,s'}^{(\tilde{Z})}(\theta^*)$ aids in identifiability of the covariance parameters (Yan et al., 2007). The caregiver dataset has replication at the location level, thus we are required to include independent error for the latent process of the ratings. For a dataset without replication, one could drop the independent error and assume

$$Z_{ij}^* = \mathbf{x}_{ij}'\beta + \tilde{Z}(s_i).$$

We constrain the total error variance of $\tilde{Z}(s)$ to be one, because an unconstrained covariance is confounded with β . The constrained covariance for the model without independent error results in the correlation function

$$\mathbf{R}_{s,s'}^{(\tilde{Z})}(\theta) = \frac{\mathbf{a}_{g(s)}' \boldsymbol{\Gamma}(s, s') \mathbf{a}_{g(s')}}{\|\mathbf{a}_{g(s)}\| \|\mathbf{a}_{g(s')}\|}.$$

Lastly, at least one of the σ_q^2 must be fixed for identifiability. When \mathbf{A} is a lower triangular matrix it is intuitive to set $\sigma_1^2 = 1$. Note that estimation of the remaining σ_q^2 for $q > 1$ is possible because we use a single set of cut points across all Q land-use categories. Allowing a different set of cut points for each land-use process would require all of the σ_q^2 s be fixed. For the first observed process, the proportion of spatial variation only depends on the first element of \mathbf{A} . When $\sigma_1^2 = 1$, the proportion of variance due to the spatial correlation, as opposed to independent error, is $\frac{a_{11}^2}{1+a_{11}^2}$, where a_{qq} is the corresponding element of \mathbf{A} . When the remaining σ_q^2 , for $q > 1$, are allowed to vary this provides greater flexibility in the cross-correlation functions for the proportion of independent error of the remaining spatial processes. Estimating the σ_q^2 can be difficult; therefore, we suggest fixing $\sigma_q^2 = 1$ for all q . We find that this assumption is not unreasonable as the free elements of the matrix \mathbf{A} provide enough flexibility to account for varying amounts of independent error for each land-use process.

3.4. Implications of the LMC specification. We now explore the implications of the LMC specification on the cross-covariance function of the multivariate latent process. Gneiting, Kleiber and Schlather (2010) note that when all elements of the matrix \mathbf{A} are treated as unknown parameters (i.e. no structural zeros), the smoothness of each latent process is determined by the roughest latent component and that by fixing the upper right elements of the matrix \mathbf{A} to be zero, distinct smoothness properties can be estimated. In a similar vein, we find that the structural zeros also help in identifying distinct spatial range parameters for each component process.

Imposing this structure of \mathbf{A} , however, does indirectly place restrictions on the cross-covariance function. Consider the setting where the dimension of the latent process, Q , is

three and \mathbf{A} is lower triangular such that $a_{qq'} = 0$ for all $q' > q$, where $a_{qq'}$ denotes the (q, q') element of \mathbf{A} . Let $\tilde{\boldsymbol{\eta}}(\mathbf{s})$ be the constrained multivariate process defined by the LMC with the constraint given in Equation 1. The cross-covariance matrix-valued function for $\tilde{\boldsymbol{\eta}}(\mathbf{s})$ and $\tilde{\boldsymbol{\eta}}(\mathbf{s}')$ can be written as

$$(2) \quad \begin{bmatrix} \frac{a_{11}^2 \rho_1}{\|\mathbf{a}_1\|^2 + \sigma_1^2} & \frac{a_{11} a_{21} \rho_1}{\sqrt{\|\mathbf{a}_1\|^2 + \sigma_1^2} \sqrt{\|\mathbf{a}_2\|^2 + \sigma_2^2}} & \frac{a_{11} a_{31} \rho_1}{\sqrt{\|\mathbf{a}_1\|^2 + \sigma_1^2} \sqrt{\|\mathbf{a}_3\|^2 + \sigma_3^2}} \\ \frac{a_{11} a_{21} \rho_1}{\sqrt{\|\mathbf{a}_1\|^2 + \sigma_1^2} \sqrt{\|\mathbf{a}_2\|^2 + \sigma_2^2}} & \frac{a_{21}^2 \rho_1 + a_{22}^2 \rho_2}{\|\mathbf{a}_2\|^2 + \sigma_2^2} & \frac{a_{21} a_{31} \rho_1 + a_{22} a_{32} \rho_2}{\sqrt{\|\mathbf{a}_1\|^2 + \sigma_1^2} \sqrt{\|\mathbf{a}_3\|^2 + \sigma_3^2}} \\ \frac{a_{11} a_{31} \rho_1}{\sqrt{\|\mathbf{a}_1\|^2 + \sigma_1^2} \sqrt{\|\mathbf{a}_3\|^2 + \sigma_3^2}} & \frac{a_{21} a_{31} \rho_1 + a_{22} a_{32} \rho_2}{\sqrt{\|\mathbf{a}_1\|^2 + \sigma_1^2} \sqrt{\|\mathbf{a}_3\|^2 + \sigma_3^2}} & \frac{a_{21}^2 \rho_1 + a_{22}^2 \rho_2 + a_{33} \rho_3}{\|\mathbf{a}_3\|^2 + \sigma_3^2} \end{bmatrix},$$

where $\rho_q = \rho(\mathbf{s}, \mathbf{s}', \phi_q)$. From this expression for the cross-correlation function in Equation 2, it is clear that the cross-covariance between the first latent process and the other two only depends on ρ_1 . That is, the structural zeros in \mathbf{A} restrict the cross-covariance function between the first and subsequent latent process to only depend on the spatial dependence structure of the first spatial process. It immediately follows that an implication of the lower-triangular form of \mathbf{A} is that the ordering of the land-use categories has implications for the cross-covariance function. Additionally, we note that ordering of the components can affect the identifiability of distinct spatial range parameters of the spatial processes. We discuss our strategy for ordering land-use categories in Section 4.

Additionally, the implied cross-covariance function from the LMC model also has implications for the trade off between independent error and spatial variance when all σ_q^2 are set to one. For each land-use process the proportion of independent error is $\frac{1}{\|\mathbf{a}_q\|+1}$. A land-use process with greater independent error will have proportionally less spatial error. Because the total error variance is constrained to one, the land-use processes $\eta_q(\mathbf{s}) + \delta_q$ will have smaller spatial variance for land-use types with a greater proportion of independent error.

3.5. Model fitting. The full Bayesian model is specified by placing priors on the covariance parameters $\boldsymbol{\theta}^*$, and mean function parameters $\boldsymbol{\delta}$ and $\boldsymbol{\beta}$. A normal prior for $\boldsymbol{\delta}$ and $\boldsymbol{\beta}$ is conditionally conjugate in the data augmented probit model. Both $\boldsymbol{\phi}$ and $\boldsymbol{\sigma}^2$ have support on the positive real line and $\text{vec}(\mathbf{A})$ on the real line.

We wrote a custom MCMC algorithm in Julia to fit the model (Bezanson et al., 2017; Rackauckas and Nie, 2017; Lin et al., 2019; Besançon et al., 2021; Frigo and Johnson, 2005; Mogensen and Riseth, 2018). As MCMC is computationally time consuming and burdensome we also propose an approximation method that does not utilize the data augmentation framework, but rather treats the ratings as a Gaussian outcome. We fit the approximate model by direct maximization of the approximate posterior. We say “approximate” as it is not appropriate to assume ordinal data follow a normal distribution, but for the AHDC collective efficacy data spatial predictions from this approximate model are nearly identical to those produced by the land-use filtering model and can be obtained much faster (computation time is hours instead of days).

To facilitate the discussion of each method used to fit the model we introduce vector notation. Let \mathbf{Y} be a $n \times 1$ vector of ratings and \mathbf{Z}^* be the $n \times 1$ latent response vector with Y_r and Z_r^* denoting the r th rating and latent variable. The vector $\tilde{\mathbf{Z}} = (\tilde{Z}_1, \dots, \tilde{Z}_m)'$ contains the spatial random effects for each location, where $\tilde{Z}_i = \tilde{Z}(\mathbf{s}_i)$. The r th row of the design matrix \mathbf{X} contains the covariates \mathbf{x}_r of the r th rating. \mathbf{H} is a $m \times n$ matrix of ones and zeros that associates the spatial random effects to the corresponding locations of each rating. The $n \times 1$ vector $\boldsymbol{\epsilon}$ of independent errors have a unique constrained variance $\tilde{\sigma}_q^2$ for each land-use type q . We then write the model as

$$\mathbf{Z}^* = \mathbf{X}\boldsymbol{\beta} + \mathbf{H}\tilde{\mathbf{Z}} + \tilde{\boldsymbol{\epsilon}},$$

where vector of spatial random effects, $\tilde{\mathbf{Z}}$, has a multivariate normal distribution,

$$\tilde{\mathbf{Z}}|\boldsymbol{\delta}, \boldsymbol{\theta}^* \sim \text{MVN}(\mathbf{M}\boldsymbol{\delta}, \tilde{\boldsymbol{\Sigma}}(\boldsymbol{\theta}^*)),$$

and \mathbf{M} is a $m \times Q$ matrix of zeros and ones that associates the i th location with the mean shift δ_q of the corresponding land-use type. Lastly, the $\tilde{\epsilon}$ are independent,

$$\tilde{\epsilon}|\boldsymbol{\theta}^* \sim \text{N}(\mathbf{0}, \tilde{\mathbf{D}}),$$

with $\tilde{\sigma}_q^2$ on the r th diagonal of $\tilde{\mathbf{D}}$ for rating r with land-use type q .

3.5.1. MCMC. To facilitate mixing of the MCMC algorithm, we integrate out the spatial random effects. After doing so, we write the model as

$$\mathbf{Z}^* = \mathbf{X}\boldsymbol{\beta} + \mathbf{M}^*\boldsymbol{\delta} + \boldsymbol{\nu},$$

with the error term $\boldsymbol{\nu}$ having a multivariate normal distribution,

$$\boldsymbol{\nu}|\boldsymbol{\theta}^* \sim \text{N}(\mathbf{0}, \mathbf{R}(\boldsymbol{\theta}^*)),$$

where $\mathbf{M}^* = \mathbf{H}\mathbf{M}$ and

$$(3) \quad \mathbf{R}(\boldsymbol{\theta}^*) = \mathbf{H}\tilde{\boldsymbol{\Sigma}}(\boldsymbol{\theta}^*)\mathbf{H}' + \tilde{\mathbf{D}}$$

is a correlation matrix. First, we update the cut points and latent vector \mathbf{Z}^* . The cut points are drawn from a uniform distribution $\gamma_k \sim \text{U}(\max(Z_r^*|Y_r = k), \min(Z_r^*|Y_r > k))$. While alternative schemes have been proposed for updating the cut points, these strategies prove to be impractical computationally for our relatively large data set in the spatial setting (Albert and Chib, 1997; Cowles, 1996; Higgs and Hoeting, 2010). Each Z_r^* in the latent vector \mathbf{Z}^* is drawn from a normal distribution obtained by conditioning on $\boldsymbol{\beta}$, $\boldsymbol{\delta}$ and all other observations \mathbf{Z}_{-r}^* and truncated to support $[\gamma_{Y_{r-1}}, \gamma_{Y_r}]$. As the precision matrix, $\boldsymbol{\Lambda} = \mathbf{R}(\boldsymbol{\theta}^*)^{-1}$, is used to evaluate the likelihood of \mathbf{Z}^* in the posterior for a Metropolis-Hastings update of $\boldsymbol{\theta}$, we also write the variance of $Z_r^*|\mathbf{Z}_{-r}^*$ in terms of the precision to avoid additional inverse calculations: $\text{var}(Z_r^*|\mathbf{Z}_{-r}^*) = 1/\boldsymbol{\Lambda}_{rr}$. After obtaining a draw of \mathbf{Z}^* , the regression coefficients $\boldsymbol{\beta}$ and mean shift $\boldsymbol{\delta}$ can be drawn jointly from their full conditional distributions with Gibbs updates. We update $\boldsymbol{\theta}$ jointly with a Metropolis-Hastings step evaluating the posterior conditional on the current draw of \mathbf{Z}^* . We use a multivariate normal proposal distribution for $\boldsymbol{\theta}$ centered around the current draw of $\boldsymbol{\theta}$. We tune the covariance matrix for the proposal by running the algorithm to obtain at least ten thousand draws with a diagonal covariance. From this initial run, we scale the covariance of the draws of $\boldsymbol{\theta}$ by 0.25 and use the resulting matrix as the covariance of our proposal distribution for the final run of the MCMC.

3.5.2. Approximate maximum a posteriori estimation. While running the full MCMC allows us to assess uncertainty in the model parameters, the algorithm is very time consuming to run due to the matrix inversions required to compute the likelihood of the latent vector \mathbf{Z}^* . As an alternative, we consider a strategy to estimate the model parameters that finds the maximum *a posteriori* estimates of parameters from a model that approximates the full Bayesian ordinal specification. The approximate model treats the outcomes as Gaussian, so that

$$\mathbf{Y}^* = \mathbf{X}\boldsymbol{\beta} + \mathbf{M}^*\boldsymbol{\delta} + \boldsymbol{\nu}$$

$$\boldsymbol{\nu}|\boldsymbol{\theta}^* \sim \text{N}(\mathbf{0}, \boldsymbol{\Sigma}(\boldsymbol{\theta}^*)),$$

where $\boldsymbol{\Sigma}(\boldsymbol{\theta}^*) = \mathbf{H}\boldsymbol{\Sigma}(\boldsymbol{\theta})\mathbf{H}' + \mathbf{D}$. The main difference between the ordinal model and the approximate model is that the covariance of $\boldsymbol{\nu}$ is unconstrained. To simplify the calculations

required to find the *a posteriori* estimates under this approximate model, we integrate out β and δ and only estimate the covariance parameters θ^* . The marginal distribution of \mathbf{Y} is then given by

$$\mathbf{Y}|\theta^* \sim \mathcal{N}(\mathbf{0}, \mathbf{X}\Sigma_\beta\mathbf{X}' + \mathbf{M}^*\Sigma_\delta\mathbf{M}^{*'} + \mathbf{H}\Sigma(\theta)\mathbf{H}' + \mathbf{D}),$$

where Σ_δ and Σ_β are the covariance from the priors placed on δ and β . We optimize for θ^* by placing priors on θ^* and then finding the maximum a posteriori estimate of the approximate marginal posterior.

3.6. Prediction of the latent collective efficacy process. While the land-use filtering model is built on the assumption that we only observe a single land-use process at each location, when making predictions we can predict the latent level of our response for all land-use categories at any location. These predictions may be useful in visualizing how the spatial processes differ from one another, however, predictions of land-use processes at locations that do not match the true land-use category may not be meaningful depending on the application at hand. It would not be correct, for our data example, to predict the change in the latent level of defense if a location changed land-use categories from residential to nonresidential.

We now detail how to obtain samples from the posterior predictive distribution for the spatial process $\tilde{Z}(\mathbf{s})$ at any location. Let \tilde{S} be the ordered set of new locations at which we want to obtain predictions of the spatial process $\tilde{Z}(\mathbf{s})$ for $\mathbf{s} \in \tilde{S}$ for a component of collective efficacy. Let $\tilde{\mathbf{M}}$ be the matrix which associates prediction locations to a land-use category. Additionally, let draws from the posterior distribution be indexed by b . To obtain a draw $\tilde{\mathbf{Z}}^{[b]}$ from the posterior predictive distribution we need to evaluate the following covariance matrices plugging in the posterior samples of model parameters (denoted by superscript $[b]$): $\tilde{\Sigma}_{\tilde{S},S}(\theta^{*[b]})$ and $\tilde{\Sigma}_{\tilde{S},\tilde{S}}(\theta^{*[b]})$ from Equation 1 and $\mathbf{R}_{S,S}(\theta^{*[b]})$ from Equation 3. Then using properties of the multivariate normal distribution, we draw $\tilde{\mathbf{Z}}^{[b]}$ from $\tilde{\mathbf{Z}}|\mathbf{Z}^{*[b]}$ from $\mathcal{N}(\boldsymbol{\mu}^{[b]}, \Sigma^{[b]})$, where

$$\begin{aligned} \boldsymbol{\mu}^{[b]} &= \tilde{\mathbf{M}}\boldsymbol{\delta}^{[b]} + \tilde{\Sigma}_{\tilde{S},S}(\theta^{*[b]})\mathbf{R}_{S,S}^{-1}(\theta^{*[b]})(\mathbf{Z}^{*[b]} - \mathbf{X}\boldsymbol{\beta}^{[b]} - \mathbf{M}^*\boldsymbol{\delta}^{[b]}) \\ \Sigma^{[b]} &= \tilde{\Sigma}_{\tilde{S},\tilde{S}}(\theta^{*[b]}) - \tilde{\Sigma}_{\tilde{S},S}(\theta^{*[b]})\mathbf{R}_{S,S}^{-1}(\theta^{*[b]})\tilde{\Sigma}_{S,\tilde{S}}(\theta^{*[b]}). \end{aligned} \tag{4}$$

The $\tilde{\mathbf{Z}}^{[b]}$ s are samples from the posterior predictive distribution $\tilde{\mathbf{Z}}|\mathcal{Y}$.

4. Analysis of the AHDC caregiver data. We fit our proposed land-use filtering ordinal regression model to the caregiver ratings, separately for each of the three components of collective efficacy. As noted in Section 3.4, the ordering of the land-use processes in the LMC specification is consequential for identifiability of distinct spatial range parameters and has implications on the cross-covariance between land-use types. From our preliminary analyses in Section 2.3, we found that the residential processes had shorter spatial range than the nonresidential latent processes. Therefore, we selected residential as the first component in the LMC specification of the multivariate process $\boldsymbol{\eta}(\mathbf{s})$ and nonresidential as the second. We then set the “other” category third, as the “other” category has very few observations (≈ 50) for all three components of collective efficacy. Moreover, we set the third latent component process in the LMC specification for the covariance function to be spatially independent (i.e. setting ϕ_3 to positive infinity) as we found that the range parameter of the third latent process, ϕ_3 , is weakly identifiable for each component and MCMC chains did not appear to converge when we attempted to estimate it. As we expect the components of collective efficacy to differ in terms of the nature of the spatial dependence structure between nonresidential and “other” land-use areas and the “other” category covers a nonnegligible portion of the city, we

could not justify collapsing the nonresidential and “other” categories into a single land-use category.

In the design matrix \mathbf{X} , we include time-of-day indicators (daytime, nighttime, or mixed) and the day-of-week indicators (weekday only, weekend only, or mixed) as reported by the survey participants. We allow the fixed effects corresponding to time-of-day and day-of-the-week to differ by land-use category. The baseline category is residential locations rated during the daytime for weekdays. For the “other” category, we collapse day-of-the-week categories weekend-only and mixed and time-of-day categories night-only and mixed due to data availability.

We placed $N(0, 10)$ priors on each of the β ’s and δ ’s, independent $N(0, 100)$ priors on the elements a_{ij} of \mathbf{A} , $\text{Cauchy}^+(0, 1)$ on each of the range parameters ϕ_i , and a flat prior on the cut points. Ordering of the cut points in the posterior is imposed by the likelihood of the latent variables. For each land-use filtering model, we ran each MCMC for 400,000 iterations discarding the first 200,000 as burn in.

4.1. Model comparison. We compare the land-use filtering model for each collective efficacy component to a model that assumes a single stationary latent process. The only difference in the models is the specification of the correlation matrix. As such, we use the same $N(0, 10)$ priors on each of the β ’s and δ ’s and a flat prior on the cut points. While the land-use filtering model defines the correlation matrix, $\mathbf{R}(\boldsymbol{\theta}^*)$, as in Equation 3, the stationary model defines the correlation as $\mathbf{R}(\bar{\boldsymbol{\theta}}) = (1 - \kappa)\mathbf{R}(\phi) + \kappa\mathbf{I}$, where $\kappa = 1/(1 + \tau^2)$, \mathbf{I} is the identity matrix, $\mathbf{R}(\phi)$ is defined using the exponential correlation function and $\bar{\boldsymbol{\theta}} = \{\phi, \tau^2\}$. We place $\text{Cauchy}^+(0, 1)$ priors on ϕ and τ^2 . As we are not interested in using predictions from the stationary model and the covariance parameters (i.e. only ϕ and τ^2) converge more quickly, we obtain 10,000 samples and discard the first 2,000 as burn in.

To compare the fitted models, we use the Widely Applicable Information Criterion (WAIC) (Watanabe, 2010). Information criteria use the log predictive density and a penalty for over fitting. In our models, the predictive density (or likelihood) for the data augmentation model is recovered by integrating out the latent variable \mathbf{Z}^* , resulting in an integral over the multi-variate normal distribution:

$$p(\mathbf{Y}|\boldsymbol{\theta}^*, \boldsymbol{\delta}, \boldsymbol{\beta}, \boldsymbol{\gamma}) = \int \cdots \int p(\mathbf{Y}, \mathbf{Z}^*|\boldsymbol{\theta}^*, \boldsymbol{\delta}, \boldsymbol{\beta}, \boldsymbol{\gamma}) d\mathbf{Z}^*.$$

WAIC is defined on the log pointwise posterior predictive density, which requires that the posterior predictive density to be factored by individual observations. In the land-use filtered model this factorization is obtained by conditioning on the spatial random effects $\tilde{\mathbf{Z}}$ in the model,

$$\begin{aligned} p(\mathbf{Y}|\boldsymbol{\theta}^*, \boldsymbol{\delta}, \boldsymbol{\beta}, \boldsymbol{\gamma}) &= \int \cdots \int p(\mathbf{Y}, \mathbf{Z}^*|\boldsymbol{\theta}^*, \tilde{\mathbf{Z}}, \boldsymbol{\beta}, \boldsymbol{\gamma}) d\mathbf{Z}^* \\ &= \int_{C_1} p(Z_1^*|\boldsymbol{\theta}^*, \tilde{\mathbf{Z}}, \boldsymbol{\beta}, \boldsymbol{\gamma}) dZ_1^* \cdots \int_{C_n} p(Z_n^*|\boldsymbol{\theta}^*, \tilde{\mathbf{Z}}, \boldsymbol{\beta}, \boldsymbol{\gamma}) dZ_n^* \\ &= \prod_{r=1}^n [\Phi(\gamma_{Y_r} - \mathbf{x}'_r \boldsymbol{\beta} - \mathbf{h}'_r \tilde{\mathbf{Z}}) - \Phi(\gamma_{Y_{r-1}} - \mathbf{x}'_r \boldsymbol{\beta} - \mathbf{h}'_r \tilde{\mathbf{Z}})], \end{aligned}$$

where $\Phi()$ is the standard normal cumulative distribution function and \mathbf{h}_r is the column vector of the r th row of \mathbf{H} . The distribution of Y_r given Z_r^* is simply the indicator function $I(\gamma_{Y_{r-1}} < Z_r^* < \gamma_{Y_r})$, which gives the above bounds of integration

$$C_r = [\gamma_{Y_{r-1}}, \gamma_{Y_r}],$$

where we define $\gamma_0 = -\infty$ and $\gamma_K = \infty$. As a post processing step of the MCMC output, we obtain samples from the posterior distribution of the spatial random effects by drawing samples from the full conditional distribution given in Equation 4 for all observed locations.

4.2. Results. We begin with a comparison of model fit using WAIC. The WAIC of the land-use filtering model and stationary model for each component of collective efficacy is given in Table 3. To calculate WAIC we drew the spatial random effect from thinned (every 8th draw after burn in for the stationary models and every 200th draw after burn in for the land-use filtering models) MCMC chains to give us 1000 draws from each model. Thinning facilitated a quicker computation of WAIC. For all three components, the WAIC is lower for the land-use filtering model, indicating a better model fit. The dimension expansion technique applied in the land-use filtering model allows us to estimate different spatial processes for each land-use type, allowing for a better fit of the underlying spatial process for each component of collective efficacy across land-use types.

TABLE 3
WAIC scores for the land-use filtering and the stationary model

	Defense	Trust	Observation
Land-use Filtering	16997.6	13210.4	17993.6
Stationary Covariance	17726.1	13911.0	18851.5

Now we discuss how parameter estimates from our land-use filtering and stationary models compare and what these estimates help us understand about the variation of collective efficacy within the I-270 belt loop. Tables 4 and 5 give the posterior mean estimates of the parameters in the land-use filtering and stationary models respectively.

The land-use filtering processes for each of the components of collective efficacy, trust, defence, and observation have a similar characterization. The residential processes (which depends only on ϕ_1 and a_{11}) are characterized by short range spatial dependence and a small proportion of independent error. For the observation process, ϕ_1 is sufficiently high that the residential ratings are practically independent. The nonresidential processes (which depends on the combination of ϕ_1 , ϕ_2 through a_{21} , and a_{22} have much longer range spatial dependence due to the greater weight a_{22} on the longer range ϕ_2 . Again, the observation component of collective efficacy estimates less spatial dependence for nonresidential locations as compared to nonresidential locations for trust and defense. For observation, a_{21} is estimated to be near zero, which indicates that the nonresidential land-use process is independent from the residential process. By separating the latent processes of the ratings into land-use categories we are better able to estimate how the processes vary within and across land-use categories. For the “other” land-use processes, the estimates of the weights are highly variable due to the very few observations in the third category. The weight a_{33} of the third component is near zero for all three components of collective efficacy, indicating that additional independent error is unnecessary for model fit. For the stationary models, the single estimate of ϕ is in between estimates of ϕ_1 and ϕ_2 from the land-use filtering model. The stationary model smooths evenly over the entire study region and masks variation by land-use category.

The regression coefficients for the two models are comparable. The baseline category is residential locations during the daytime and weekdays. The only credible intervals that do not contain zero across all three components are the nighttime coefficients for residential locations. For all three components, we estimate a lower level in the latent process (i.e. higher probability of a lower rating) for residential locations at night. We are able to estimate this effect as caregivers were asked to rate their home neighborhood on all three components of

TABLE 4

Posterior mean estimates and corresponding posterior 95% credible intervals of the parameters in the land-use filtered Bayesian ordinal regression model. The numeric subscripts for the β 's and δ 's correspond to the land-use processes: 1 for residential, 2 for nonresidential, 3 for the "other" category. Note, with the LMC, the subscripts for the $a_{qq'}$'s correspond to the linear weights that relate the independent component processes $w_q(\mathbf{s})$, each with spatial range ϕ_q , to the multivariate outcome $\eta(\mathbf{s})$. For example, the residential process is defined by a_{11} and ϕ_1 , the nonresidential process is defined by a_{21} , a_{22} , ϕ_1 and ϕ_2 . The third component process $w_3(\mathbf{s})$ is spatially independent, thus ϕ_3 is fixed at positive infinity. The subscripts "tod" and "dow" stand for time of day and day of week with "n" for night, "m" for mixed, and "e" for weekend.

	Trust		Defense		Observation	
	Posterior mean	95% Credible interval	Posterior mean	95% Credible interval	Posterior mean	95% Credible interval
ϕ_1	404.97	(334, 488)	330.71	(264, 408)	1971.74	(1185, 3524)
ϕ_2	23.32	(11.1, 40.4)	2.83	(0.48, 8.51)	92.20	(57.9, 136.5)
a_{11}	1.79	(1.65, 1.94)	1.40	(1.25, 1.55)	1.62	(1.49, 1.75)
a_{21}	0.31	(0.18, 0.43)	0.31	(0.21, 0.40)	0.05	(-0.12, 0.19)
a_{22}	0.70	(0.58, 0.81)	0.58	(0.46, 0.71)	0.34	(0.29, 0.39)
a_{31}	1.01	(-0.22, 2.43)	-0.49	(-5.44, 3.91)	0.43	(-0.73, 1.70)
a_{32}	0.71	(-0.21, 1.70)	-0.06	(-5.06, 4.78)	0.63	(-0.09, 1.46)
a_{33}	-0.03	(-1.63, 1.58)	0.07	(-7.12, 7.64)	0.01	(-1.55, 1.60)
δ_2	-0.11	(-0.54, 0.31)	0.06	(-0.75, 0.85)	0.01	(-0.11, 0.17)
δ_3	-0.09	(-0.60, 0.43)	-0.00	(-0.92, 0.89)	0.11	(-0.28, 0.50)
$\beta_{1,tod=n}$	-0.21	(-0.26, -0.16)	-0.41	(-0.47, -0.35)	-0.17	(-0.22, -0.12)
$\beta_{1,tod=m}$	-0.13	(-0.27, 0.01)	0.09	(-0.04, 0.22)	0.14	(0.00, 0.29)
$\beta_{1,dow=e}$	0.32	(0.11, 0.54)	0.15	(-0.01, 0.32)	-0.16	(-0.33, 0.03)
$\beta_{1,dow=m}$	0.31	(0.17, 0.45)	-0.01	(-0.11, 0.10)	-0.24	(-0.33, -0.11)
$\beta_{2,tod=n}$	-0.07	(-0.17, 0.02)	-0.03	(-0.11, 0.06)	-0.12	(-0.21, -0.03)
$\beta_{2,tod=m}$	-0.04	(-0.13, 0.06)	0.01	(-0.07, 0.09)	0.01	(-0.08, 0.11)
$\beta_{2,dow=e}$	-0.02	(-0.11, 0.08)	-0.06	(-0.14, 0.02)	-0.23	(-0.33, -0.14)
$\beta_{2,dow=m}$	-0.01	(-0.10, 0.07)	-0.04	(-0.11, 0.04)	-0.11	(-0.19, -0.03)
$\beta_{3,tod=n/m}$	-0.00	(-0.77, 0.78)	-0.20	(-0.81, 0.41)	-0.01	(-0.70, 0.68)
$\beta_{3,dow=e/m}$	-0.14	(-0.85, 0.56)	-0.09	(-0.69, 0.50)	-0.36	(-1.01, 0.27)
γ_1	-1.69	(-1.82, -1.52)	-1.87	(-1.98, -1.76)	-2.14	(-2.23, -2.00)
γ_2	-1.04	(-1.16, -0.89)	-1.28	(-1.37, -1.19)	-1.47	(-1.55, -1.32)
γ_3	-0.14	(-0.26, -0.00)	-0.54	(-0.61, -0.45)	-0.45	(-0.51, -0.31)
γ_4	0.99	(0.85, 1.13)	0.69	(0.62, 0.80)	0.44	(0.38, 0.57)

collective efficacy for both the daytime and the nighttime. For nonresidential and "other" locations, we do not explicitly have this counterfactual information in the data set. Additionally, we estimate a positive effect for the weekend and day-of-week-mixed effects for residential locations for the trust component in both the land-use filtering model and stationary model. Lastly, we note that there is little evidence that the mean shifts for each land-use category are not zero in the land-use filtering model as the credible intervals all contain zero. The credible intervals for mean shift effects which do not contain zero in the stationary model may arise due to the over smoothing across land-use categories because of the stationary covariance function.

4.3. *Predictions.* Visualization of the predicted levels of each component of collective efficacy also supports the use of the land-use filtering model. Figure 5 contains the point-wise posterior mean predictions of the spatial random effect $\tilde{\mathbf{Z}}$ across a fine grid of points

TABLE 5

Estimated posterior means and corresponding posterior 95% credible intervals of the parameters in the stationary Bayesian ordinal regression model. The numeric subscripts for the β 's and δ 's correspond to the land-use processes: 1 for residential, 2 for nonresidential, 3 for the "other" category. The subscripts "tod" and "dow" stand for time of day and day of week with "n" for **n**ight, "m" for **m**ixed, and "e" for **w**eekend.

	Trust		Defense		Observation	
	Posterior mean	95% Credible interval	Posterior mean	95% Credible interval	Posterior mean	95% Credible interval
ϕ	129.86	(96.1, 166.9)	102.75	(68.1, 141.9)	493.57	(343.6, 689.6)
τ^2	0.78	(0.65, 0.92)	0.35	(0.27, 0.43)	0.31	(0.23, 0.38)
δ_2	-0.10	(-0.21, 0.02)	0.10	(0.00, 0.21)	0.12	(0.05, 0.19)
δ_3	-0.02	(-0.40, 0.37)	0.11	(-0.24, 0.45)	0.09	(-0.27, 0.44)
$\beta_{1,tod=n}$	-0.19	(-0.26, -0.12)	-0.41	(-0.48, -0.33)	-0.16	(-0.24, -0.09)
$\beta_{1,tod=m}$	-0.11	(-0.26, 0.04)	0.11	(-0.03, 0.25)	0.16	(0.01, 0.31)
$\beta_{1,dow=e}$	0.25	(0.06, 0.44)	0.14	(-0.04, 0.31)	-0.09	(-0.25, 0.07)
$\beta_{1,dow=m}$	0.29	(0.19, 0.40)	0.01	(-0.09, 0.11)	-0.15	(-0.22, -0.08)
$\beta_{2,tod=n}$	-0.08	(-0.17, 0.01)	-0.04	(-0.13, 0.05)	-0.12	(-0.21, -0.03)
$\beta_{2,tod=m}$	-0.03	(-0.12, 0.06)	0.01	(-0.08, 0.10)	0.01	(-0.08, 0.11)
$\beta_{2,dow=e}$	-0.02	(-0.12, 0.07)	-0.06	(-0.14, 0.03)	-0.23	(-0.32, -0.14)
$\beta_{2,dow=m}$	0.00	(-0.08, 0.09)	-0.00	(-0.08, 0.07)	-0.10	(-0.18, -0.02)
$\beta_{3,tod=n/m}$	-0.15	(-0.93, 0.63)	-0.11	(-0.82, 0.60)	0.01	(-0.71, 0.73)
$\beta_{3,dow=e/m}$	-0.16	(-0.83, 0.52)	0.04	(-0.61, 0.68)	-0.45	(-1.09, 0.21)
γ_1	-1.70	(-1.74, -1.63)	-1.94	(-1.99, -1.90)	-2.05	(-2.12, -1.97)
γ_2	-1.06	(-1.08, -1.02)	-1.33	(-1.36, -1.30)	-1.37	(-1.43, -1.33)
γ_3	-0.16	(-0.17, -0.14)	-0.54	(-0.56, -0.53)	-0.33	(-0.35, -0.31)
γ_4	1.00	(0.94, 1.03)	0.76	(0.73, 0.79)	0.57	(0.55, 0.58)

(over 100,000) within the I-270 belt loop. The land-use category of each prediction location was assigned by the land-use category of the nearest parcel. We obtained predictions using Equation 4 for each of the draws of the thinned MCMC chains used in the WAIC calculations. Plotted is the point-wise posterior mean of the spatial random effect ($\mu^{[b]}$ in Equation 4) at each prediction location averaged across the thinned draws. We calculated the posterior mean of the spatial random effect rather than the mean of posterior predictive distribution due to memory constraints for obtaining a multivariate normal sample at a very fine grid of locations. The fine grid of locations allows us to better visualize within neighborhood variation across land-use categories. The predicted stationary process on the right is more smooth compared to the predicted land-use process on the left. Land-use filtering allows use to estimate distinct processes for each land-use type while also smoothing over land-use boundaries. There are discontinuities in the prediction at the boundaries from one land-use type to another, however, these discontinuities would be greater if we simply fit three independent process (i.e. the matrix of weights \mathbf{A} is a diagonal matrix) for each land-use category and then filtered the processes. The predicted land-use filtered process for the defense and trust components shows the shorter range spatial dependence within residential areas and the longer range spatial dependence for non-residential locations. For the observation component, the spatial range of residential locations is effectively zero, thus the predictions revert to the mean for residential locations while allowing for greater spatial smoothing over nonresidential locations.

As the full Bayesian spatial ordinal regression model is time consuming to fit we also compared the predictions from the ordinal land-use filtering model to predictions from the approximate land-use filtering model described in Section 3.5.2. The approximate model

treats the rating response directly as a Gaussian outcome, thus the scales of predictions are different. Additionally, treating the outcome directly as Gaussian allows one to drop the restrictions on the covariance function when defining the land-use filtering process. Predictions from both models are very highly correlated for each component of collective efficacy: predictions for the defense component had a correlation of 0.98, for trust a correlation of 0.97, and for observation a correlation of 0.96. In practice, when uncertainty estimates of the collective efficacy process are not needed, using the approximate model will give nearly the same results as the full Bayesian spatial ordinal model with a significant reduction in computation time.

5. Discussion. As demonstrated in the previous section, our proposed land-use filtering model for the AHDC collective efficacy data better fits the observed data than the default approach using a spatial generalized linear model with a single stationary latent process. This superiority holds for all three components of collective efficacy. Due to the lack of software for fitting alternative models with a single nonstationary latent process, as opposed to the default latent stationary model discussed in Section 4, our model comparison exercise is somewhat limited in scope. For example, [Risser and Calder \(2015\)](#)’s covariance-regression model could be used to allow the parameters of the latent spatial process to vary smoothly with spatially-referenced land-use covariate information.

Another limitation of our analysis is that we were not able to account for dependence in the collective efficacy component ratings made by the same individual. Conceptually, it may be possible to account for differences in how individuals use the component response scales since individuals report on several locations, which may be rated by multiple individuals. However, since many routine locations will be closer to the caregiver’s home location, we found that an individual random effect is essentially confounded with the spatial random effect. Since the latter is of primary interest and necessary for spatial prediction at unrated locations, we decided to forego an individual-level random effect in our analyses.

Finally, we note that our prediction of the collective efficacy components across the study area implicitly assume that the caregivers who rate locations other than their residence are a representative sample of individuals who frequent the locations as part of their daily routine. We view this assumption as foundational to our notion of collective efficacy as a continuously-indexed spatial process. Alternatively, one could define collective efficacy of a location from the perspective of an objective observer, who may or may not spend time at the location. This notion is not compatible with the AHDC Study design and, more importantly, is arguably not consistent with sociological theory which emphasizes perceptions of space among users of the space.

In future work, we will use the estimated continuously-indexed spatial collective efficacy component processes to examine the relationship between collective efficacy and point-level crime data. We will also explore the hypothesis that within-neighborhood variation in collective efficacy relates to crime ([Weisburd et al., 2016](#)). Such an analysis is only possible with our fine-grained maps of collective efficacy across the study area.

In conclusion, while our proposed land-use filtering model is a novel method for learning about small-scale variability in collective efficacy across an urban environment, we acknowledge that the approach may be more generally applicable. Other spatial prediction problems in which the spatial dependence structure may depend on land use (e.g., pollution mapping) might benefit from the modeling approach. More broadly, any spatially-dependent, categorical variable that defines a partition of a well-defined study area could be used instead of land use in the approach.

Funding. This study was supported in part by the National Institute on Drug Abuse (Christopher R. Browning; R01DA032371); the Eunice Kennedy Shriver National Institute on Child Health and Human Development (Catherine A. Calder; R01HD088545; John Cast-erline, The Ohio State University Institute for Population Research, P2CHD058484; Elizabeth Gershoff, The University of Texas at Austin Population Research Center, P2CHD-042849); and the W. T. Grant Foundation.

SUPPLEMENTARY MATERIAL

Example dataset and code

AHDC data will be deposited to Inter-university Consortium for Political and Social Research (ICPSR) in publicly available and restricted access forms (expected in Summer 2022). To ensure participant privacy and maintenance of data confidentiality, the ADHC caregiver location reports needed to reproduce the analyses in this paper will only be available in the restricted access version of the data. Qualified researchers will be able to submit an application to ICPSR for access to the data. In our supplementary material, we instead provide a synthetic data set generated from the posterior predictive distribution of the trust component at randomly selected locations out of the grid of points used for our predictive maps. Accompanying the example data set is code to reproduce the analyses done in the paper.

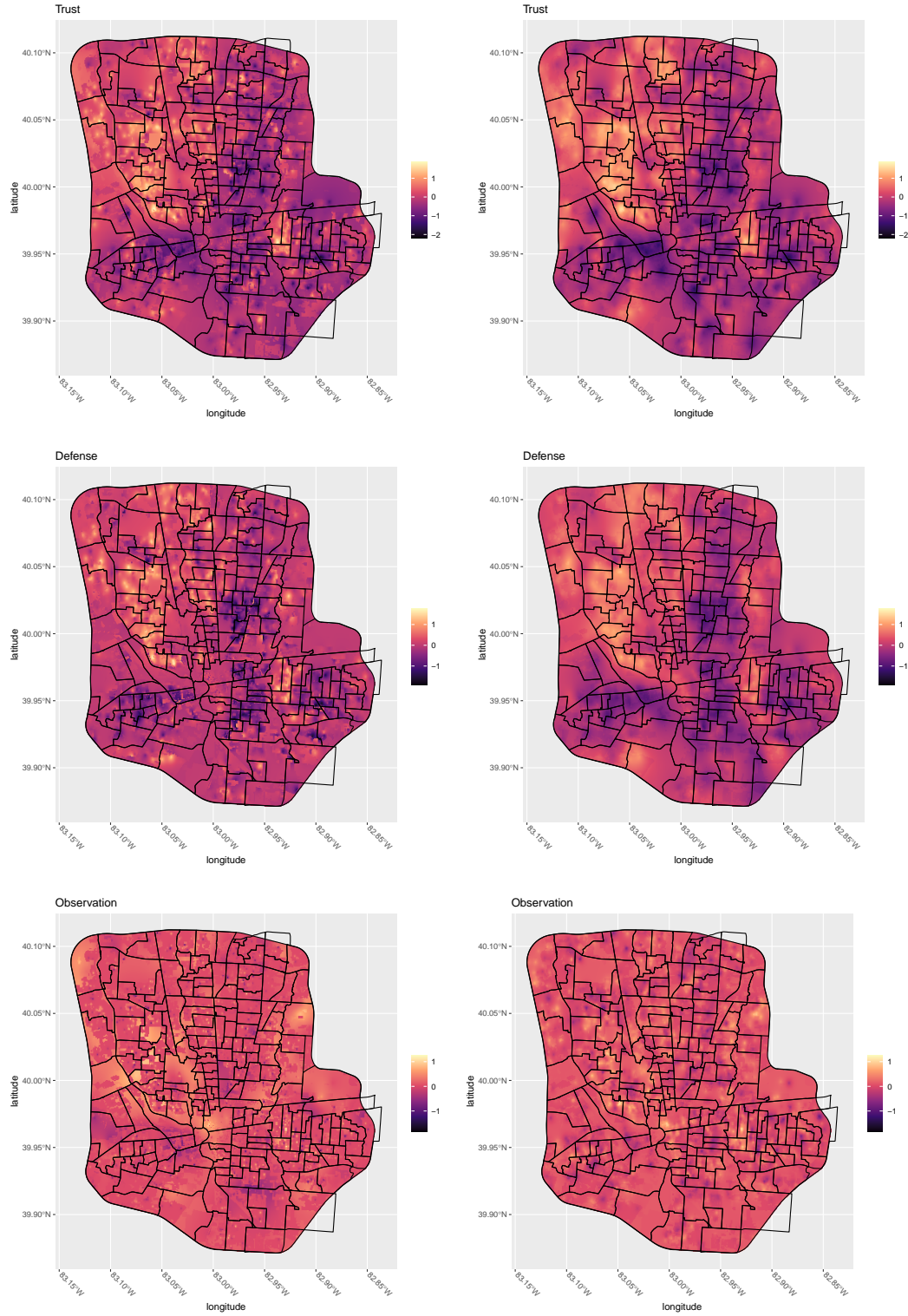


FIG 5. Point-wise posterior means of the spatial random effects for trust (top row), defense (middle row), and observation (bottom row). On the left are the predictions of the collective efficacy components derived from the land-use filtering model. Predictions from the stationary model are on the right. The scales are the same for plots on the same row.

REFERENCES

- ALBERT, J. H. and CHIB, S. (1993). Bayesian analysis of binary and polychotomous response data. *Journal of the American Statistical Association* **88** 669–679.
- ALBERT, J. and CHIB, S. (1997). Bayesian methods for cumulative, sequential and two-step ordinal data regression models.
- APANASOVICH, T. V., GENTON, M. G. and SUN, Y. (2012). A valid Matérn class of cross-covariance functions for multivariate random fields with any number of components. *Journal of the American Statistical Association* **107** 180–193.
- FRANKLIN COUNTY AUDITOR (2021). Franklin county GIS parcel shape files. 2014 Data retrieved from <https://franklincountyauditor.com/ftp>.
- BANDURA, A. (1982). Self-efficacy mechanism in human agency. *The American psychologist* **37** 122–147.
- BANDURA, A. (1986). *Social foundations of thought and action : a social cognitive theory* / Albert Bandura. Prentice-Hall series in social learning theory. Prentice-Hall, Englewood Cliffs, N.J.
- BANERJEE, S., CARLIN, B. P. and GELFAND, A. E. (2014). *Hierarchical modeling and analysis for spatial data*, Second ed. Chapman and Hall/CRC, New York. <https://doi.org/10.1201/b17115>
- BERRETT, C. and CALDER, C. A. (2012). Data augmentation strategies for the Bayesian spatial probit regression model. *Computational Statistics & Data Analysis* **56** 478–490.
- BERRETT, C. and CALDER, C. A. (2016). Bayesian spatial binary classification. *Spatial Statistics* **16** 72–102. <https://doi.org/10.1016/j.spasta.2016.01.004>
- BESANÇON, M., PAPAMARKOU, T., ANTHOFF, D., ARSLAN, A., BYRNE, S., LIN, D. and PEARSON, J. (2021). Distributions.jl: Definition and modeling of probability distributions in the JuliaStats ecosystem. *Journal of Statistical Software* **98** 1–30. <https://doi.org/10.18637/jss.v098.i16>
- BEZANSON, J., EDELMAN, A., KARPINSKI, S. and SHAH, V. B. (2017). Julia: A fresh approach to numerical computing. *SIAM review* **59** 65–98.
- BORNN, L., SHADDICK, G. and ZIDEK, J. (2012). Modeling non-stationary processes through dimension expansion. *Journal of the American Statistical Association* **107** 281–289. <https://doi.org/10.1080/01621459.2011.646919>
- BROWNING, C. R. (2002). The span of collective efficacy: Extending social disorganization theory to partner violence. *Journal of marriage and family* **64** 833–850.
- CALDER, C. A. (2008). A dynamic process convolution approach to modeling ambient particulate matter concentrations. *Environmetrics* **19**. <https://doi.org/10.1002/env.852>
- COHEN, D. A., FINCH, B. K., BOWER, A. and SASTRY, N. (2006). Collective efficacy and obesity: The potential influence of social factors on health. *Social science & medicine (1982)* **62** 769–778.
- COLEMAN, J. S. (1988). Social capital in the creation of human capital. *American journal of sociology* **94** S95–S120.
- CORCORAN, J., ZAHNOW, R., WICKES, R. and HIPPI, J. (2018). Neighbourhood land use features, collective efficacy and local civic actions. *Urban studies (Edinburgh, Scotland)* **55** 2372–2390.
- COWLES, M. K. (1996). Accelerating Monte Carlo Markov chain convergence for cumulative-link generalized linear models. *Statistics and Computing* **6** 101–111.
- DE OLIVEIRA, V. (1997). Prediction in some classes of non-Gaussian random fields, PhD thesis, University of Maryland, College Park.
- DE OLIVEIRA, V. (2000). Bayesian prediction of clipped Gaussian random fields. *Computational Statistics & Data Analysis* **34** 299–314.
- FRIGO, M. and JOHNSON, S. G. (2005). The design and implementation of FFTW3. *Proceedings of the IEEE* **93** 216–231. Special issue on “Program Generation, Optimization, and Platform Adaptation”. <https://doi.org/10.1109/JPROC.2004.840301>
- GELFAND, A. E., SCHMIDT, A. M., BANERJEE, S. and SIRMANS, C. F. (2004). Nonstationary multivariate process modeling through spatially varying coregionalization. *Test (Madrid, Spain)* **13** 263–312.
- GNEITING, T., KLEIBER, W. and SCHLATHER, M. (2010). Matérn cross-covariance functions for multivariate random fields. *Journal of the American Statistical Association* **105** 1167–1177.
- GOULARD, M. and VOLTZ, M. (1992). Linear coregionalization model: Tools for estimation and choice of cross-variogram matrix. *Mathematical geology* **24** 269–286.
- GRZEBYK, M. and WACKERNAGEL, H. (1994). Multivariate analysis and spatial/temporal scales: Real and complex models. In *Proceedings of the XVIIth International Biometrics Conference* **1** 19–33. Citeseer.
- HIGGS, M. D. and HOETING, J. A. (2010). A clipped latent variable model for spatially correlated ordered categorical data. *Comput. Stat. Data Anal.* **54** 1999–2011. <https://doi.org/10.1016/j.csda.2010.02.024>
- INGEBRIGTSEN, R., LINDGREN, F. and STEINSLAND, I. (2014). Spatial models with explanatory variables in the dependence structure. *Spatial Statistics* **8** 20–38.
- JACOBS, J. (1961). *The death and life of great American cities*. Random House, New York.

- LIN, D., WHITE, J. M., BYRNE, S., BATES, D., NOACK, A., PEARSON, J., ARSLAN, A., SQUIRE, K., ANTHOFF, D., PAPAMARKOU, T., BESANÇON, M., DRUGOWITSCH, J., SCHAUER, M. and CONTRIBUTORS (2019). JuliaStats/Distributions.jl: a Julia package for probability distributions and associated functions. <https://doi.org/10.5281/zenodo.2647458>
- MATSUEDA, R. L. and DRAKULICH, K. M. (2016). Measuring collective efficacy: A multilevel measurement model for nested data. *Sociological methods & research* **45** 191-230.
- MOGENSEN, P. K. and RISETH, A. N. (2018). Optim: A mathematical optimization package for Julia. *Journal of Open Source Software* **3** 615. <https://doi.org/10.21105/joss.00615>
- MOLNAR, B. E., GOERGE, R. M., GILSANZ, P., HILL, A., SUBRAMANIAN, S. V., HOLTON, J. K., DUNCAN, D. T., BEATRIZ, E. D. and BEARDSLEE, W. R. (2015). Neighborhood-level social processes and substantiated cases of child maltreatment. *Child abuse & neglect* **51** 41-53.
- NETO, J. H. V., SCHMIDT, A. M. and GUTTORP, P. (2014). Accounting for spatially varying directional effects in spatial covariance structures. *Journal of the Royal Statistical Society. Series C (Applied Statistics)* **63** 103-122.
- PEBESMA, E. (2018). Simple features for R: standardized support for spatial vector data. *The R Journal* **10** 439-446. <https://doi.org/10.32614/RJ-2018-009>
- RACKAUCKAS, C. and NIE, Q. (2017). DifferentialEquations.jl – A performant and feature-rich ecosystem for solving differential equations in Julia. *The Journal of Open Research Software* **5**. Exported from <https://app.dimensions.ai> on 2019/05/05. <https://doi.org/10.5334/jors.151>
- RAUDENBUSH, S. W. and SAMPSON, R. J. (1999). Ecometrics: Toward a science of assessing ecological settings, with application to the systematic social observation of neighborhoods. *Sociological methodology* **29** 1-41.
- REICH, B. J., EIDSVIK, J., GUINDANI, M., NAIL, A. J. and SCHMIDT, A. M. (2011). A class of covariate-dependent spatiotemporal covariance functions. *The annals of applied statistics* **5** 2265-2687.
- RISSER, M. D. and CALDER, C. A. (2015). Regression-based covariance functions for nonstationary spatial modeling. *Environmetrics*. **26**.
- RISSER, M. D., CALDER, C. A., BERROCAL, V. J. and BERRETT, C. (2019). Nonstationary spatial prediction of soil organic carbon: Implications for stock assessment decision making. *The Annals of Applied Statistics*.
- SAMPSON, R. J., RAUDENBUSH, S. W. and EARLS, F. (1997). Neighborhoods and violent crime: A multilevel study of collective efficacy. *Science* **277** 918-924. <https://doi.org/10.1126/science.277.5328.918>
- SCHLIEP, E. M. and HOETING, J. A. (2015). Data augmentation and parameter expansion for independent or spatially correlated ordinal data. *Computational statistics & data analysis* **90** 1-14.
- SCHMIDT, A. M., GUTTORP, P. and O'HAGAN, A. (2011). Considering covariates in the covariance structure of spatial processes. *Environmetrics*. **22**.
- SHAW, C. R. and MCKAY, H. D. (1942). *Juvenile delinquency and urban areas*. University of Chicago Press, Chicago, Ill.
- R CORE TEAM (2022). R: A language and environment for statistical computing R Foundation for Statistical Computing, Vienna, Austria.
- WACKERNAGEL, H. (2003). *Multivariate geostatistics : an introduction with applications / Hans Wackernagel.*, 3rd, completely rev. ed. ed. Springer, Berlin ;.
- WATANABE, S. (2010). Asymptotic equivalence of Bayes cross validation and widely applicable information criterion in singular Learning Theory. *Journal of Machine Learning Research* **11** 3571-3594.
- WEISBURD, D., ECK, J. E., BRAGA, A. A., TELEP, C. W., CAVE, B., BOWERS, K., BRUINSMA, G., GILL, C., GROFF, E. R., HIBDON, J. and ET AL. (2016). *Place matters: Criminology for the twenty-first century*. Cambridge University Press. <https://doi.org/10.1017/CBO9781139342087>
- WICKES, R., ZAHNOW, R., CORCORAN, J. and HIPPI, J. R. (2019). Neighbourhood social conduits and resident social cohesion. *Urban studies (Edinburgh, Scotland)* **56** 226-248.
- WICKHAM, H., AVERICK, M., BRYAN, J., CHANG, W., MCGOWAN, L. D., FRANÇOIS, R., GROLEMUND, G., HAYES, A., HENRY, L., HESTER, J., KUHN, M., PEDERSEN, T. L., MILLER, E., BACHE, S. M., MÜLLER, K., OOMS, J., ROBINSON, D., SEIDEL, D. P., SPINU, V., TAKAHASHI, K., VAUGHAN, D., WILKE, C., WOO, K. and YUTANI, H. (2019). Welcome to the tidyverse. *Journal of Open Source Software* **4** 1686. <https://doi.org/10.21105/joss.01686>
- YAN, J., COWLES, M. K., WANG, S. and ARMSTRONG, M. P. (2007). Parallelizing MCMC for Bayesian spatiotemporal geostatistical models. *Statistics and Computing* **17** 323-335.